Progress In Electromagnetics Research, PIER 89, 291–310, 2009

FAR FIELD RADIATION FROM AN ARBITRARILY ORIENTED HERTZIAN DIPOLE IN AN UNBOUNDED ELECTRICALLY GYROTROPIC MEDIUM

A. Eroglu

Department of Engineering
Indiana University-Purdue University
Fort Wayne, IN 46805-1499, USA

J. K. Lee

Department of Electrical Engineering and Computer Science
Syracuse University
Syracuse, NY 13244-1240, USA

Abstract—The solution to the problem of far field radiation from an arbitrarily oriented Hertzian dipole in an electrically gyrotropic medium is found with the application of dyadic Green's function (DGF) technique. The form of the DGF, which is expressed as the sum of two single dyads, simplifies the derivation of the far fields significantly in comparison to the existing methods. The far field integral is evaluated analytically using the method of steepest descent. The numerical results for the radiation fields are presented in different frequency bandwidth using Clemmow-Mually-Allis (CMA) diagram. It is shown that the operational frequency bandwidth and the orientation of the antenna, which give the highest directivity and gain, can be determined when the CMA diagram is employed. Our analytical results are compared with the existing ones which were obtained using different techniques. Agreement is observed on all of them. The results presented in this paper can be used for radiation problems involving space exploration, radio astronomy or laboratory plasmas.

Corresponding author: A. Eroglu (Email: eroglua@ipfw.edu).

1. INTRODUCTION

The electromagnetic radiation from an electric Hertzian dipole in an electrically gyrotropic or gyroelectric medium such as magnetically biased cold plasma is very important for radio propagation problems in space explorations and some problems in laboratory plasmas.

Bunkin [1] calculated the radiation fields of Hertzian dipole when it is placed in a gyroelectric medium such as cold plasma using a tensorial Green's function in index notation with employing differential operators. In his paper, the magnetostatic field was assumed to be in z-direction. He only presented analytical results and expressed the far field components in the Cartesian coordinate system. Wu [2] and Felsen [3] formulated the same problem as an eigenfunction expansion. Some of the numerical results when the electric dipole is directed in x direction can be found in [2]. Clemmow [4] used the idea of angular spectrum of plane waves. His method can be used when the source current is confined to a plane and flows parallel to that plane. He gave only analytical results in the limiting case assuming the magnetic field in the plasma is so strong that the medium can be considered as a uniaxial plasma. Al'pert and Moiseyev [5] solved the problem of dipole radiation from a homogeneous magnetoactive plasma in all the resonance frequency ranges by using Fourier-Bessel functions as a solution of second order derivatives of electric and magnetic fields.

In this paper, we solve the problem of far field radiation from an unbounded electrically gyrotropic medium when the applied magnetic field is in z-direction. We use the method of dyadic Green's functions [6] in spectral domain. The new form of the dyadic Green's function (DGF) for a gyroelectric medium [7] is used. Since DGF is expressed as a sum of two single dyads, it significantly facilitates the analytical calculation of the far fields in comparison to the existing methods. The complete set of far field components is analytically derived using the method of steepest descents and put in a simple form. CMA diagram [8] is utilized to investigate the radiation characteristics of Hertzian dipole in different frequency bandwidths. We show that the CMA diagram can be used in the radiation problems involving gyroelectric medium such as cold plasma to obtain information about the key parameters of the problem. For instance, our method can be used to determine acceptable frequency bandwidth and the orientation of the antenna to have the highest directivity and gain. Our results are compared with the existing results. Agreement has been observed on all of them.

2. FORMULATION AND SOLUTIONS

The medium under consideration is an electrically gyrotropic or gyroelectric medium such as cold plasma and described by a relative permittivity tensor in a dyadic form as

$$\bar{\bar{\varepsilon}} = \varepsilon_1 \left(\bar{\bar{I}} - \hat{b}_0 \hat{b}_0 \right) + i\varepsilon_2 \left(\hat{b}_0 \times \bar{\bar{I}} \right) + \varepsilon_3 \hat{b}_0 \hat{b}_0 \tag{1}$$

$\hat{b}_0$ shows the direction of the applied dc magnetic field $\bar{B}_o$. It is assumed that fields are time-harmonic with $e^{-i\omega t}$ dependence. When $\bar{B}_0 \equiv \hat{b}_0 B_0 = \hat{z} B_0$, i.e., $\hat{b}_0 = \hat{z} = (0, 0, 1)$, the relative permittivity tensor, $\bar{\bar{\varepsilon}}$, takes the following form in matrix notation

$$\bar{\bar{\varepsilon}} = \begin{bmatrix} \varepsilon_1 & -i\varepsilon_2 & 0 \\ i\varepsilon_2 & \varepsilon_1 & 0 \\ 0 & 0 & \varepsilon_3 \end{bmatrix} \tag{2}$$

The elements of $\bar{\bar{\varepsilon}}$ are defined as

$$\varepsilon_1 = 1 - \frac{X_0}{1 - Y_0^2} = 1 - \frac{\omega_p^2}{\omega^2 - \omega_b^2} \tag{3}$$

$$\varepsilon_2 = -\frac{X_0 Y_0}{1 - Y_0^2} = -\frac{\omega_b \omega_p^2}{\omega \left(\omega^2 - \omega_b^2 \right)} \tag{4}$$

$$\varepsilon_3 = 1 - X_0 = 1 - \frac{\omega_p^2}{\omega^2} \tag{5}$$

$$\omega_b = \frac{eB_0}{m} \tag{6}$$

$$\omega_p = \left(\frac{N_0 e^2}{m\varepsilon_0} \right)^{1/2} \tag{7}$$

where $X_0 = \frac{\omega_p^2}{\omega^2}$ and $Y_0 = \frac{\omega_b}{\omega}$. ω_b is called the gyrofrequency or cyclotron frequency and ω_p is called the plasma frequency. N_0 shows the number of free electrons per unit volume, and m represents the mass of each electron with charge $-e$. The permeability of the medium is assumed to be $\mu_0 = 4\pi \times 10^{-7}$ [H/m].

The geometry of the medium when the applied external magnetic field is in z-direction with an arbitrary direction of a wave vector $\bar{k}$ is shown in Fig. 1.

We consider the problem of a far field radiation from an unbounded gyroelectric medium when the dipole is located at the origin as shown in Fig. 2.

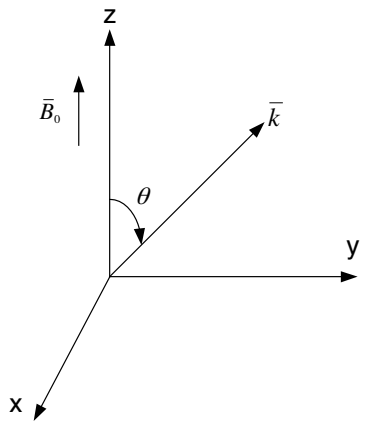

Figure 1. Wave propagation in an electrically gyrotropic medium with an arbitrary direction of $\bar{k}$ and applied magnetostatic field $\bar{B}_0$.

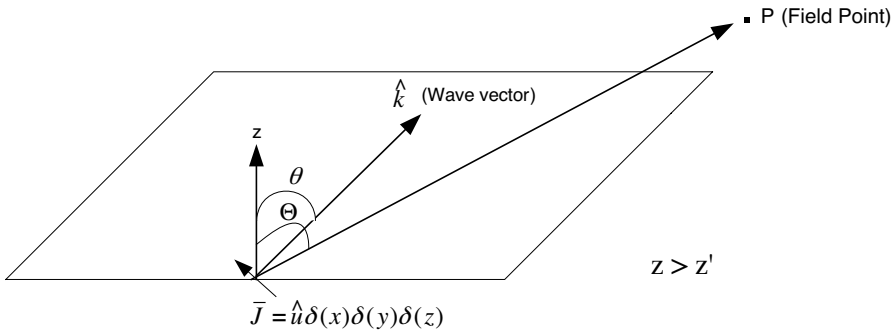

Figure 2. The geometry of the problem when the dipole is located at the origin.

The dyadic Green's function (DGF) for an unbounded gyroelectric medium satisfies the following wave equation with the radiation condition at infinity

$$\left[\nabla \times \nabla \times \bar{\bar{I}} - k_0^2 \bar{\bar{\varepsilon}}\right] \cdot \bar{\bar{G}}_{ee}^{e}\left(\bar{r}, \bar{r}'\right) = i\omega\mu_0 \bar{\bar{I}} \delta\left(\bar{r} - \bar{r}'\right) \tag{8}$$

The superscript of the DGF, $\bar{\bar{G}}_{ee}^{e}(\bar{r}, \bar{r}')$, refers to the type of the gyrotropic medium, which is electrically gyrotropic in this case, and the first and the second subscripts show the type of the DGF. The subscript 'e' refers to the electric type DGF. DGF, $\bar{\bar{G}}_{ee}^{e}(\bar{r}, \bar{r}')$, in (8) is

derived in [7] as

$$\bar{\bar{G}}^{e}_{ee}\left(\bar{r},\bar{r}'\right)=\frac{-\omega\mu_0}{8\pi^2}\int\limits_{-\infty}^{\infty}\int\limits_{-\infty}^{\infty}dk_xdk_y$$
$$\left\{\begin{array}{r}\frac{1}{k_0^2\varepsilon_3\left(k_{zI}^2-k_{zII}^2\right)}\left[\frac{\alpha_I}{k_{zI}}\hat{e}_{nI}\left(k_{zI}\right)\hat{e}^{*}_{nI}\left(k_{zI}\right)e^{i\bar{k}_I\cdot\left(\bar{r}-\bar{r}'\right)}\right.\\ \left.-\frac{\alpha_{II}}{k_{zII}}\hat{e}_{nII}\left(k_{zII}\right)\hat{e}^{*}_{nII}\left(k_{zII}\right)e^{i\bar{k}_{II}\cdot\left(\bar{r}-\bar{r}'\right)}\right]\end{array}\right\},\ z>z' \quad (9)$$

The two dimensional spectral form of the DGF in (9) is obtained after performing the integration over k_z by assuming the medium to be slightly lossy, i.e., $\mathrm{Im}k_z \ll \mathrm{Re}k_z$, $\mathrm{Im}k_z > 0$. This guarantees that the radiation condition is satisfied at $z = \pm\infty$. In Equation (9), α_I and α_{II} are the eigenvalues, $\hat{e}_{nI}(\pm k_{zI})$ and $\hat{e}_{nII}(\pm k_{zI})$ are the orthonormal eigenvectors, which physically represent two characteristic electric fields for the type I and II waves that exist in a gyroelectric medium. α_i, k_i, k_{zi}, $\hat{e}_{ni}(k_{zi})$ where $i = I, II$ are given in Appendix A. The parameters with the subscript $i = I$ refer to type I wave and those with the subscript $i = II$ refer to type II wave. Type I and type II waves are the waves that can exist in a gyroelectric medium and their propagation and dispersion characteristics are discussed in detail in [8]. The wave vectors and corresponding wave numbers are defined as

$$\bar{k}_i = \bar{k}_\rho + \hat{z}k_{zi}, \quad i = I, II \quad (10)$$
$$k_i^2 = k_\rho^2 + k_{zi}^2 = k_x^2 + k_y^2 + k_{zi}^2, \quad i = I, II \quad (11)$$

To calculate the far field radiation of a dipole from an unbounded gyroelectric medium, the far field approximated DGF for $z > z'$ has to be found for the problem shown in Fig. 2. In the same region, the electric field $\bar{E}$ satisfies

$$\nabla\times\nabla\times\bar{E}\left(\bar{r}\right)-k_0^2\bar{\bar{\varepsilon}}\cdot\bar{E}\left(\bar{r}\right)=i\omega\mu_0\bar{J}\left(\bar{r}\right) \quad (12)$$

The electric field radiated by a Hertzian dipole can be calculated by using the the DGF:

$$\bar{E}(\bar{r})=\int_{V'}\bar{\bar{G}}^{e}_{ee}\left(\bar{r},\bar{r}'\right)\cdot\bar{J}\left(\bar{r}'\right)d^3\bar{r}' \quad (13)$$

where

$$\bar{J}\left(\bar{r}'\right)=\hat{u}c\delta\left(x'\right)\delta\left(y'\right)\delta\left(z'\right) \quad (14)$$

In Equation (14), c is the current moment of the electric dipole, which is defined as $\int I(z)dz$ for a linear antenna, and $\hat{u}$ is the orientation of the dipole. Under the far field approximation, the integral in (9) can be evaluated using the method of steepest descent [9, 10] as $r \to \infty$. We assume that the dipole is located at the origin, i.e., $\bar{r}' = 0$. We can rewrite the equation in (9) by splitting it into type I and II components as

$$\bar{\bar{G}}^{e}_{ee}\left(\bar{r}, \bar{r}'\right) = I_1 - I_2 \tag{15}$$

where

$$I_1 = \int\int_{-\infty}^{\infty} e^{i\bar{k}_\rho \cdot \bar{\rho}} \bar{\bar{F}}_I\left(\bar{k}_\rho\right) dk_x dk_y \tag{16}$$

$$I_2 = \int\int_{-\infty}^{\infty} e^{i\bar{k}_\rho \cdot \bar{\rho}} \bar{\bar{F}}_{II}\left(\bar{k}_\rho\right) dk_x dk_y \tag{17}$$

and

$$\bar{\bar{F}}_I\left(\bar{k}_\rho\right) = \frac{-\omega\mu_0}{8\pi^2} \frac{1}{k_{zI}} \frac{1}{k_0^2 \varepsilon_3 \left(k_{zI}^2 - k_{zII}^2\right)} \left[\alpha_I \hat{e}_{nI} \hat{e}^*_{nI} e^{ik_{zI}z}\right] \tag{18}$$

$$\bar{\bar{F}}_{II}\left(\bar{k}_\rho\right) = \frac{-\omega\mu_0}{8\pi^2} \frac{1}{k_{zII}} \frac{1}{k_0^2 \varepsilon_3 \left(k_{zI}^2 - k_{zII}^2\right)} \left[\alpha_{II} \hat{e}_{nII} \hat{e}^*_{nII} e^{ik_{zII}z}\right] \tag{19}$$

Please note that for simplicity in the notation we assumed $\bar{\rho}$ for $\bar{\rho} - \bar{\rho}'$ and z for $z - z'$. We did not use the notation double overbar (=) on I_1 and I_2 although they are dyadics. Since the calculations for I_1 and I_2 are similar, we will only present the analytical calculations for I_1.

We first represent the integral in (16) in cylindrical waveform by applying the following transformations.

$$\bar{k}_\rho = \hat{x} k_\rho \cos\alpha + \hat{y} k_\rho \sin\alpha \tag{20}$$

$$\bar{\rho} = \hat{x}\rho\cos\phi + \hat{y}\rho\sin\phi \tag{21}$$

$$dk_x dk_y = k_\rho dk_\rho d\alpha \tag{22}$$

So

$$\bar{k}_\rho \cdot \bar{\rho} = k_\rho \rho \cos(\alpha - \varphi) \tag{23}$$

Substituting (20)–(22) into (16) gives

$$I_1 = \int_0^{\infty} k_\rho \bar{\bar{F}}_I(k_\rho) dk_\rho \int_0^{2\pi} d\alpha e^{ik_\rho \rho \cos(\alpha - \phi)} \tag{24}$$

Using the integral identity for Bessel functions [11],

$$J_0(k_\rho\rho) = \frac{1}{2\pi}\int_0^{2\pi} d\alpha e^{ik_\rho\rho\cos(\alpha-\phi)} \tag{25}$$

and their relation with Hankel functions [12],

$$J_0(k_\rho\rho) = \frac{1}{2}\left[H_0^{(1)}(k_\rho\rho) + H_0^{(2)}(k_\rho\rho)\right] \tag{26}$$

equation in (24) can be written as

$$I_1 = \pi\int_0^{\infty} k_\rho\bar{\bar{F}}_I(k_\rho)\left[H_0^{(1)}(k_\rho\rho)\right]dk_\rho + \pi\int_0^{\infty} k_\rho\bar{\bar{F}}_I(k_\rho)\left[H_0^{(2)}(k_\rho\rho)\right]dk_\rho \tag{27}$$

By changing the variable of the integration in (27)

$$k_\rho = e^{-i\pi}k'_\rho \tag{28}$$

and using the reflection formula for Hankel functions [13],

$$H_0^{(2)}\left(e^{-i\pi}\lambda\right) = -H_0^{(1)}(\lambda) \tag{29}$$

we can express (27) in terms of the Hankel function of first kind, which is chosen to represent an outgoing wave using the "i" notation as

$$I_1 = \pi\int_{-\infty}^{\infty} k_\rho\bar{\bar{F}}_I(k_\rho)H_0^{(1)}(k_\rho\rho)dk_\rho \tag{30}$$

Substituting (18) into (30) gives

$$I_1 = \int_{-\infty}^{\infty} g(k_\rho)e^{ik_{zI}z}\frac{k_\rho}{k_{zI}}H_0^{(1)}(k_\rho\rho)dk_\rho \tag{31}$$

where

$$g(k_\rho) = \frac{-\omega\mu_0}{8\pi k_0^2\varepsilon_3}\left(\frac{\alpha_I\hat{e}_{nI}\hat{e}^*_{nI}}{k_{zI}^2 - k_{zII}^2}\right) \tag{32}$$

In (31), a plane wave propagating in the z-direction is in product with the Hankel function of first kind, which represents a cylindrical

wave propagating in ρ direction. It is scaled with an amplitude factor $g(k_\rho)$.

Because $k_{zI} = \left[k_I^2 - k_\rho^2\right]^{1/2}$ is a double valued function of k_ρ, the integral in (31) has branch point singularity at $k_\rho = \pm k_I$. $H_0^{(1)}(\lambda)$ also has a branch point singularity when $\lambda = 0$. Hence the integral in (31) is undefined unless the path of integration is identified. The typical path of integration for the integral type in (31) is the Sommerfeld integration path, Γ on complex k_ρ plane as shown in Fig. 3. On this plane, the branch point singularities $\pm k_I$ have been displaced slightly from the real axis to signify the presence of loss to satisfy the radiation condition. To facilitate the solution for the integral in (31), it is convenient to transform the complex wavenumber variable k_ρ to a complex angle variable β. The transformation can be done as follows.

$$k_\rho = k_I \sin\beta \tag{33}$$

$$k_{zI} = k_I \cos\beta \tag{34}$$

β is the complex angle between the wave normal and the z-axis and expressed as

$$\beta = \beta_r + i\beta_i \tag{35}$$

We also introduce the following transformations in polar coordinates as

$$\rho = r \sin\Theta \tag{36}$$

$$z = r \cos\Theta \tag{37}$$

Substituting (33)–(37) into (31), we obtain

$$I_1 = \int_P g(k_I \sin\beta) \tan\beta H_0^{(1)}\left(k_I r \sin\beta \sin\Theta\right) \left\{k_I' \sin\beta + k_I \cos\beta\right\} e^{ik_I r \cos\beta \cos\Theta} d\beta \tag{38}$$

where $k_I' = \frac{\partial k_I}{\partial \beta}$. P is the integration path in the complex β domain. As seen from (38), the branch point singularities at $\pm k_I$ are removed by application of the transformations shown in (33)–(37).

When the large argument approximation is applied to Hankel function of first kind in (38), i.e., $k_1 r \sin\Theta \gg 1$ and the integration path is deformed away from the origin sufficiently to assure

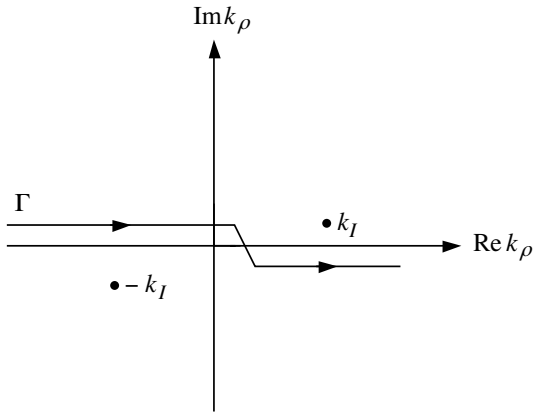

Figure 3. The integration path for I_1 on complex k_ρ plane.

$k_I r \sin\Theta \sin\beta \gg 1$ along the path P, the first order asymptotic approximation of $H_0^{(1)}$ can be written as

$$H_0^{(1)}(k_I r \sin\beta \sin\Theta) = \sqrt{\frac{2}{\pi k_I r \sin\beta \sin\Theta}} e^{i\left(k_I r \sin\beta \sin\Theta - \frac{\pi}{4}\right)} \tag{39}$$

When (39) is inserted into (38), we obtain

$$I_1 = \left(\frac{-\omega\mu_0}{8\pi k_0^2 \varepsilon_3}\right) e^{-i\frac{\pi}{4}} \sqrt{\frac{2}{\pi r \sin\Theta}} \int_P h(\beta) e^{ik_I r \cos(\beta-\Theta)} d\beta \tag{40}$$

where

$$h(\beta) = \frac{(k_I' \sin\beta + k_I \cos\beta)}{\cos\beta} \sqrt{\frac{\sin\beta}{k_I}} \left(\frac{\alpha_I \hat{e}_{nI} \hat{e}_{nI}^*}{k_{zI}^2 - k_{zII}^2}\right) \tag{41}$$

The integral in (40) is solved by using the method of the steepest descent technique [9, 10]. The integration path P is deformed into the steepest descent path by setting the imaginary part of the exponent to be equal to its value at the saddle point. When the integral in (40) is solved by using the steepest descent technique, we obtain

$$I_1 = \left(\frac{-\omega\mu_0}{4\pi k_0^4}\right) \frac{e^{ik_I r \cos(\beta_s - \Theta)}}{r} \left\{ \left[\frac{\cos\Theta}{\sqrt{\sin\Theta}} \frac{1}{\cos(\beta_s)\cos(\beta_s - \Theta)} (\alpha_I \hat{e}_{nI} \hat{e}_{nI}^*)_{\beta=\beta_s} \right] \cdot \left[\frac{\sin\beta_s k_I(\beta_s)}{\left[\cos(\beta_s - \Theta)[k_I''(\beta_s) - k_I(\beta_s)] - 2k_I'(\beta_s)\sin(\beta_s - \Theta)\right]} \right]^{1/2}$$

$$\cdot \left[\frac{k_I^4(\beta_s)}{k_0^4}\sin^4(\beta_s)(\varepsilon_1-\varepsilon_3)^2+4\varepsilon_2^2\varepsilon_3\left[\varepsilon_3-\frac{k_I^2(\beta_s)}{k_0^2}\sin^2(\beta_s)\right]\right]^{-1/2}\Bigg\} \quad (42a)$$

Repeating the same procedure for the integral I_2 in (17), we obtain

$$I_2 = \left(\frac{-\omega\mu_0}{4\pi k_0^4}\right)\frac{e^{ik_{II}r\cos(\beta_s-\Theta)}}{r}\left\{\left[\frac{\cos\Theta}{\sqrt{\sin\Theta}}\frac{1}{\cos(\beta_s)\cos(\beta_s-\Theta)}(\alpha_{II}\hat{e}_{nII}\hat{e}^*_{nII})_{\beta=\beta_s}\right]\right.$$
$$\cdot\left[\frac{\sin\beta_s k_{II}(\beta_s)}{\left[\cos(\beta_s-\Theta)[k''_{II}(\beta_s)-k_{II}(\beta_s)]-2k'_{II}(\beta_s)\sin(\beta_s-\Theta)\right]}\right]^{1/2}$$
$$\left.\cdot\left[\frac{k_{II}^4(\beta_s)}{k_0^4}\sin^4(\beta_s)(\varepsilon_1-\varepsilon_3)^2+4\varepsilon_2^2\varepsilon_3\left[\varepsilon_3-\frac{k_{II}^2(\beta_s)}{k_0^2}\sin^2(\beta_s)\right]\right]^{-1/2}\right\} \quad (42b)$$

Hence the far field approximated DGF $\bar{\bar{G}}^e_{ee}(\bar{r},\bar{r}')$ for an electrically gyrotropic medium can be expressed as in Equation (15) where I_1 and I_2 are given in (42).

The radiation fields can be found by substituting (15) and (42) into (13) as follows.

$$\bar{E}(\bar{r}) = \int_V \bar{\bar{G}}^e_{ee}(\bar{r},\bar{r}')\cdot\bar{J}(\bar{r}')\,d\bar{r}' = \bar{\bar{G}}^e_{ee}(\bar{r},\bar{r}')\Big|\cdot\hat{u}c \qquad x'=0,\quad y'=0,\quad z'=0 \quad (43a)$$

So,

$$\bar{E}(\bar{r}) = \left(\frac{-\omega\mu_0}{4\pi k_0^4}\right)\frac{e^{ik_{I,II}r\cos(\beta_s-\Theta)}}{r}$$
$$\cdot\left\{\left[\frac{\cos\Theta}{\sqrt{\sin\Theta}}\frac{1}{\cos(\beta_s)\cos(\beta_s-\Theta)}\left(\alpha_{I,II}\hat{e}_{nI,II}\hat{e}^*_{nI,II}\right)_{\beta=\beta_s}\right]\right.$$
$$\cdot\left[\frac{\sin\beta_s k_{I,II}(\beta_s)}{\left[\cos(\beta_s-\Theta)\left[k''_{I,II}(\beta_s)-k_{I,II}(\beta_s)\right]-2k'_{I,II}(\beta_s)\sin(\beta_s-\Theta)\right]}\right]^{1/2}$$
$$\left.\cdot\left[\frac{k_{I,II}^4(\beta_s)}{k_0^4}\sin^4(\beta_s)(\varepsilon_1-\varepsilon_3)^2+4\varepsilon_2^2\varepsilon_3\left[\varepsilon_3-\frac{k_{I,II}^2(\beta_s)}{k_0^2}\sin^2(\beta_s)\right]\right]^{-1/2}\right\}$$
$$\cdot\ \hat{u}c\Big|_{x'=0,y'=0,z'=0} \quad (43b)$$

We define the following variables to simplify the expressions for the radiation fields.

$$E = \left[\frac{\cos\Theta}{\sqrt{\sin\Theta}}\frac{1}{\cos(\beta_s)\cos(\beta_s-\Theta)}\right] \tag{44}$$

$$R = \left[\frac{\sin\beta_s k_{I,II}(\beta_s)}{\left[\cos(\beta_s-\Theta)\left[k''_{I,II}(\beta_s)-k_{I,II}(\beta_s)\right]-2k'_{I,II}(\beta_s)\sin(\beta_s-\Theta)\right]}\right]^{1/2} \tag{45}$$

$$O = \left[\frac{k^4_{I,II}(\beta_s)}{k^4_0}\sin^4(\beta_s)(\varepsilon_1-\varepsilon_3)^2+4\varepsilon_2^2\varepsilon_3\left[\varepsilon_3-\frac{k^2_{I,II}(\beta_s)}{k^2_0}\sin^2(\beta_s)\right]\right]^{-1/2} \tag{46}$$

$$\Re = ERO \tag{47}$$

When the dipole is oriented in $\hat{z}$ direction, $\hat{u}=\hat{z}$, the components of the radiation fields in the Cartesian coordinate system are

$$E_{iI,II} = \left(\frac{-\omega\mu_0}{4\pi k_0^4}\right)\frac{e^{ik_{I,II}r\cos(\beta_s-\Theta)}}{r}(\Re)\left(\begin{array}{c} A_{i3} \end{array}\right)_{\beta=\beta_s}, \quad i=1,2,3 \quad \text{or} \quad x,y,z \tag{48}$$

The coefficients $A_{ij},(i,j)=1,2,3$ are evaluated at $k_z=k_{zI},k_{zII}$ and defined in Appendix A by Equations (A11)–(A19). When the dipole is oriented in $\hat{y}$ direction, $\hat{u}=\hat{y}$, the components of the radiation fields in the Cartesian coordinate system are

$$E_{iI,II} = \left(\frac{-\omega\mu_0}{4\pi k_0^4}\right)\frac{e^{ik_{I,II}r\cos(\beta_s-\Theta)}}{r}(\Re)\left(\begin{array}{c} A_{i2} \end{array}\right)_{\beta=\beta_s}, \quad i=1,2,3 \quad \text{or} \quad x,y,z \tag{49}$$

When the dipole is oriented in $\hat{x}$ direction, $\hat{u}=\hat{x}$, the components of the radiation fields in the Cartesian coordinate system are

$$E_{iI,II} = \left(\frac{-\omega\mu_0}{4\pi k_0^4}\right)\frac{e^{ik_{I,II}r\cos(\beta_s-\Theta)}}{r}(\Re)\left(\begin{array}{c} A_{i1} \end{array}\right)_{\beta=\beta_s}, \quad i=1,2,3 \quad \text{or} \quad x,y,z \tag{50}$$

Our analytical results for the radiation fields given by (48)–(50) are compared with the existing results which were obtained using different techniques analytically. Radiation fields given in [1] by Equation (5.2)

agrees with our results given by (48)–(50). In [1], tensorial Green's function is represented using index notation and differential operators are introduced and used to solve the radiation problem. Our derivation uses direct notation and dyadic Green's function is expressed as the sum of two single dyads in the spectral domain. Hence in our case, a straightforward use of DGF with Equation (13) leads to solution for the radiation fields. Besides, there are no numerical results presented in [1].

3. NUMERICAL RESULTS AND DISCUSSION

In this section, the radiation patterns of $\hat{\theta}$ and $\hat{\phi}$ components for type I and II waves are obtained on the $\phi = 0^\circ$ plane when the dipole is oriented in z- and x-directions. We analyze the radiation patterns in three different regions on the CMA diagram [8]. The regions are chosen such that wave propagation exists for three cases. Namely, wave propagation can exist for both type I and II waves, or only for type I wave, or only for type II wave. Among eight regions of the CMA diagram, we will consider Regions 1, 2, and 4 to obtain the radiation characteristics of the waves to represent three cases.

3.1. Radiation in Region 1

The wave normal surface in this region is given in Fig. 4.

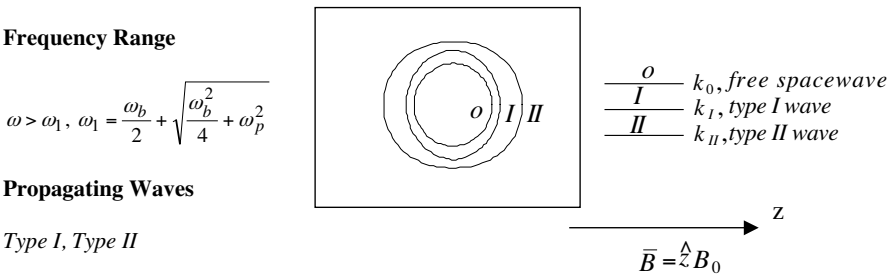

Figure 4. Wave normal surface in Region 1 when $X = 0.44$, $Y = 0.37$.

Region 1 corresponds to a high frequency region. Based on the wave normal surface given in Fig. 4, both type I and II waves propagate in this region. Hence, both types of waves are expected to radiate when the frequency of the operation falls within the specified frequency range above. The radiation patterns for $\hat{\theta}$ and $\hat{\phi}$ components of the $\bar{E}$ field for z-directed dipole on x-z plane are shown in Figs. 5(a) and 5(b),

respectively. When the dipole is z-directed, the radiation due to type I wave is stronger than type II wave for both $\hat{\theta}$ and $\hat{\phi}$ components.

The $\hat{\theta}$ component of the radiation field for type I wave has the maximum radiation at $\theta = 54.9°$. It has one symmetrical major lobe with respect to $\theta = 90°$. The minimum radiation occurs at $\theta = 0°$ for type I wave. Type II wave has two symmetrical lobes with respect to $\theta = 90°$ and the maximum radiation occurs at $\theta = 39.6°$. The minimum radiation is at $\theta = 0°, 90°$ for type II wave. When there is maximum radiation for both types of waves, the ratio of their magnitudes is $|E_{\theta I}|/|E_{\theta II}| = 2.96$.

The $\hat{\phi}$ component of the radiation field for type I wave has the maximum radiation at $\theta = 39.6°$. It has two symmetrical lobes with respect to $\theta = 90°$. The minimum radiation is at $\theta = 0°, 90°$ for type I wave. Type II wave has also two symmetrical lobes with respect to $\theta = 90°$. It has maximum radiation at $\theta = 47.1°$. The minimum radiation occurs at $\theta = 0°, 90°$. When there is maximum radiation for both types of waves, the ratio of their magnitudes is $|E_{\phi I}|/|E_{\phi II}| = 1.79$.

When the dipole is oriented in x direction, the radiation patterns for $\hat{\theta}$ and $\hat{\phi}$ components of the $\bar{E}$ field are shown in Fig. 6. The radiation strength of the $\hat{\theta}$ component for type I and II waves is almost equivalent. It resembles to a radiation pattern of a dipole in an isotropic plasma. The radiation pattern of $\hat{\phi}$ component for type I wave is more directive than type II wave.

$\hat{\theta}$ component of the radiation field for both type I and II waves

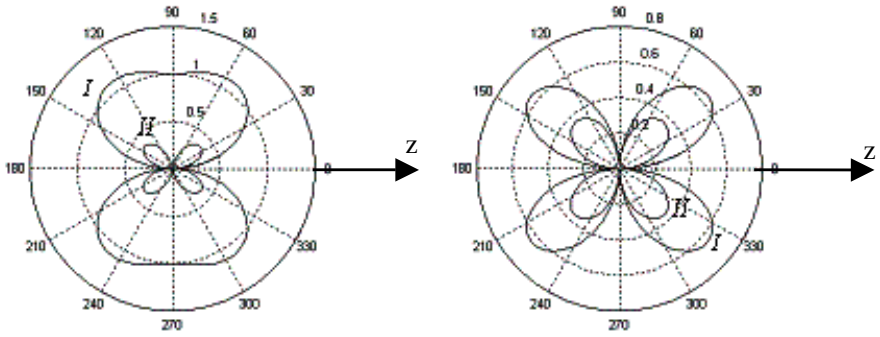

(a) (b)

Figure 5. (a) E_θ component of the radiation field for z-directed dipole on the x-z plane. (b) E_ϕ component of the radiation field for z-directed dipole on the x-z plane.

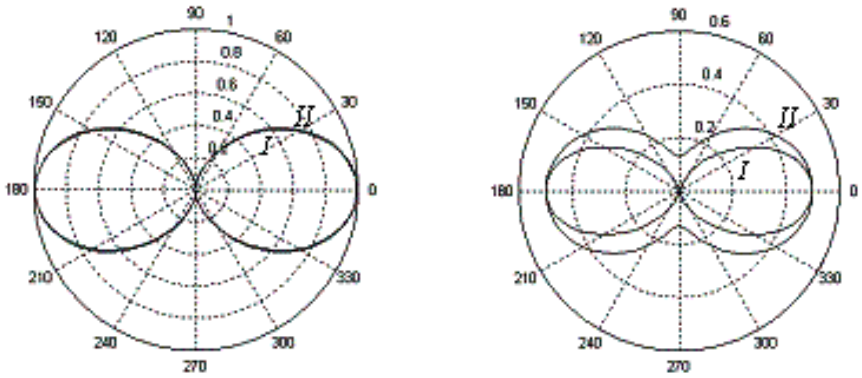

(a) (b)

Figure 6. (a) E_θ component of the radiation field for x-directed dipole on the x-z plane. (b) E_ϕ component of the radiation field for x-directed dipole on the x-z plane.

has its maximum radiation at $\theta = 0°$. It has symmetrical radiation pattern with respect to $\theta = 90°$. Minimum radiation occurs at $\theta = 90°$ for both type I and II waves. When there is maximum radiation, the ratio of their magnitudes is $|E_{\theta I}|/|E_{\theta II}| = 1.02$.

$\hat{\phi}$ component of the radiation field for both type I and II waves has its maximum radiation at $\theta = 0°$. It has symmetrical radiation pattern with respect to $\theta = 90°$. Minimum radiation for both waves is at $\theta = 90°$. Although type I wave does not radiate when $\theta = 90°$, type II wave radiates in all directions. When there is a maximum radiation for both types of waves, the ratio of their magnitudes is $|E_{\phi I}|/|E_{\phi II}| = 1.01$.

3.2. Radiation in Region 2

The wave normal surface in this region is given in Fig. 7.

In Region 2, only type I wave can propagate. As a result, radiation in this region is possible only due to type I wave. The radiation patterns for $\hat{\theta}$ and the $\hat{\phi}$ components of the $\bar{E}$ field for z-directed dipole on x-z plane are shown in Figs. 8(a) and 8(b), respectively. The radiation pattern of $\hat{\theta}$ component for the z-directed dipole carries the characteristics of the radiation pattern of a dipole in uniaxial plasma.

When the dipole is z-directed, the $\hat{\theta}$ component of the radiation field for type I wave has the maximum radiation at $\theta = 90°$. It has one major lobe, which has minimum radiation at $\theta = 0°$. $\hat{\phi}$ component of

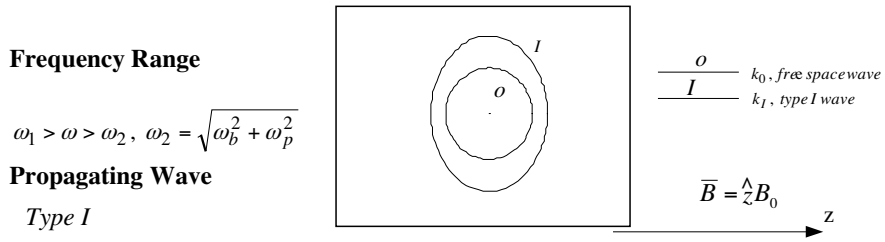

Figure 7. Wave normal surface in Region 2 when $X = 0.6083$ and $Y = 0.4386$.

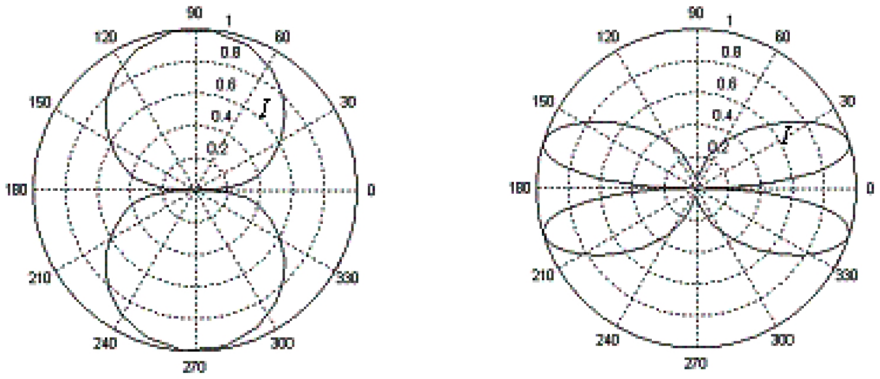

Figure 8. (a) E_θ component of the radiation field for z-directed dipole on the x-z plane. (b) E_ϕ component of the radiation field for z-directed dipole on the x-z plane.

type I wave has symmetrical lobes with respect to $\theta = 90°$. Maximum radiation occurs at $\theta = 17.1°$. Minimum radiation for type II wave is at $\theta = 0°, 90°$.

When the dipole is oriented in x direction, the radiation patterns for $\hat{\theta}$ and $\hat{\phi}$ components for type I wave has narrow beamwidth and hence antenna is very directive in this region. The radiation patterns for $\hat{\theta}$ and $\hat{\phi}$ components of the $\bar{E}$ field when the dipole is oriented in the x-direction are shown in Fig. 9.

The $\hat{\theta}$ and $\hat{\phi}$ components of the radiation field for type I waves have the maximum radiation at $\theta = 0°$. They have symmetrical radiation pattern with respect to $\theta = 90°$. The minimum radiation occurs at $\theta = 90°$ for both components.

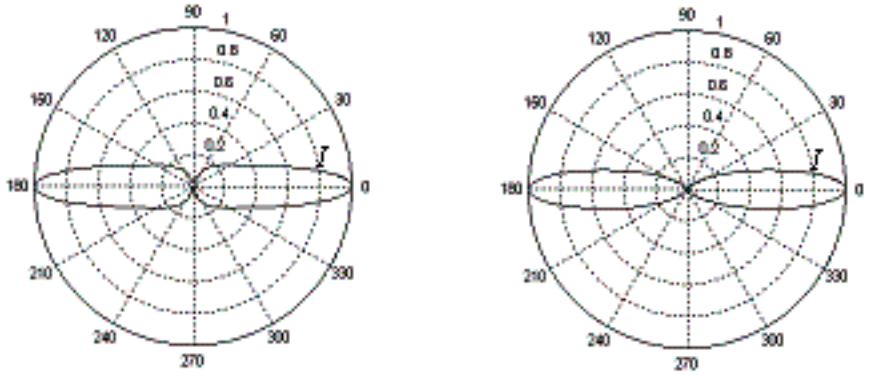

(a) (b)

Figure 9. (a) E_θ component of the radiation field for x-directed dipole on the x-z plane. (b) E_ϕ component of the radiation field for x-directed dipole on the x-z plane.

3.3. Radiation in Region 4

The wave normal surface in this region is given in Fig. 10.

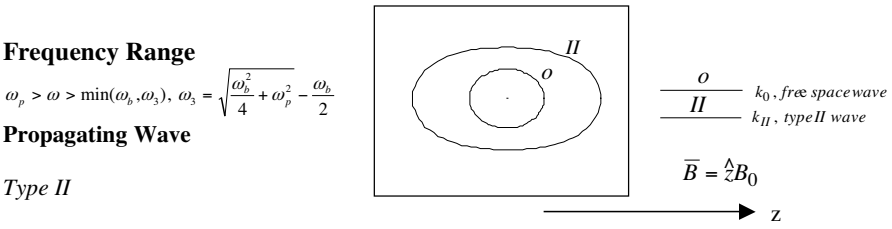

Figure 10. Wave normal surface in Region 4 when $X = 1.5041$ and $Y = 0.6897$.

In Region 4, only type II wave can propagate. So the radiation can occur only due to type II wave in this region. The radiation patterns for $\hat{\theta}$ and $\hat{\phi}$ components of the $\bar{E}$ field for the z-directed dipole on x-z plane are shown in Figs. 11(a) and 11(b), respectively. The radiation patterns for $\hat{\theta}$ and $\hat{\phi}$ components have the same radiation characteristics for the z-directed dipole in this region. Nevertheless, each lobe for $\hat{\theta}$ component is slightly more directive than the ones for $\hat{\phi}$ component of the radiation field.

When the dipole is z-directed, the $\hat{\theta}$ component of the radiation

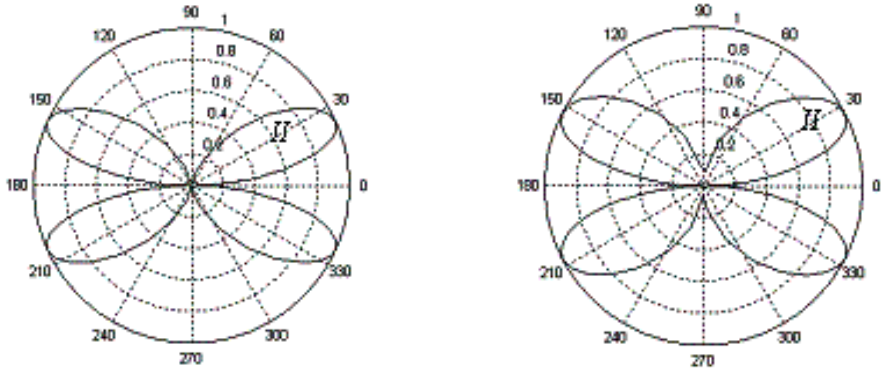

(a) (b)

Figure 11. (a) E_θ component of the radiation field for z-directed dipole on the x-z plane. (b) E_ϕ component of the radiation field for z-directed dipole on the x-z plane.

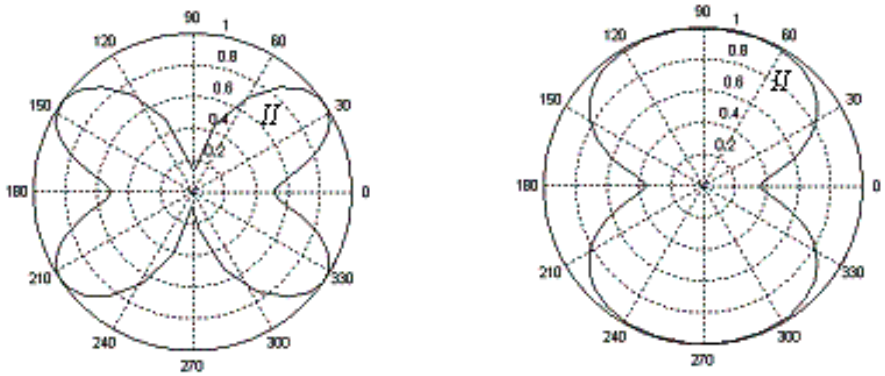

(a) (b)

Figure 12. (a) E_θ component of the radiation field for x-directed dipole on the x-z plane. (b) E_ϕ component of the radiation field for x-directed dipole on the x-z plane.

field for type II wave has the maximum radiation at $\theta = 24.1°$. It has the symmetrical radiation pattern with respect to $\theta = 90°$. The $\hat{\phi}$ component of type II waves has also symmetrical lobes with respect to $\theta = 90°$. The maximum radiation occurs at $\theta = 27.5°$. The minimum radiation is at $\theta = 0°, 90°$ for both waves.

When the dipole is oriented in x direction, the radiation patterns for the $\hat{\theta}$ component and the $\hat{\phi}$ component of the $\bar{E}$ field are shown in

Fig. 12. Antenna radiates in all directions for both components in this case.

The $\hat{\theta}$ component of the radiation field for type II wave has the maximum radiation at $\theta = 31.6°$. It has the symmetrical radiation pattern with respect to $\theta = 90°$. The $\hat{\phi}$ component of type II wave has one major lobe which has the maximum radiation occurs at $\theta = 90°$. The minimum radiation occurs at $\theta = 90°, 0°$ for $\hat{\theta}$ component and $\theta = 0°$ for $\hat{\phi}$ component.

As a final note, we can also investigate the radiation characteristics of the waves in other regions of the CMA diagram using the same technique.

4. CONCLUSION

The far field radiation of an arbitrarily oriented Hertzian dipole embedded in an unbounded gyroelectric medium is derived analytically using the DGF method. The dyadic Green's function of the medium, which is expressed as the sum of two single dyads, greatly facilitated the derivation of the far fields. The far field components are calculated using the steepest descent technique. The final results are expressed in a simple form. We used the CMA diagram as a tool to obtain the numerical results for the radiation fields in different frequency bandwidths. This helps the physical interpretation of the radiation patterns and gives us a forecast for the type of the waves that can radiate in the operating frequency region. This technique can be used to determine the key design parameters such as orientation of an antenna and the operational frequency for the radiation problems involving space applications, radio astronomy, and laboratory plasmas.

APPENDIX A.

The parameters used in (7), α_i, k_i, k_{zi}, $\hat{e}_{ni}(k_{zi})$ where $i = 1, 2$, are derived in [6] as

$$\alpha_I = k_I^4 - k_I^2 k_0^2 \left[\varepsilon_1\left(3-\cos^2\theta\right)+\varepsilon_3\left(1+\cos^2\theta\right)\right] + k_0^4\left(\varepsilon_1^2-\varepsilon_2^2+2\varepsilon_1\varepsilon_3\right) \quad \text{(A1)}$$

$$\alpha_{II} = k_{II}^4 - k_{II}^2 k_0^2 \left[\varepsilon_1\left(3-\cos^2\theta\right)+\varepsilon_3\left(1+\cos^2\theta\right)\right] + k_0^4\left(\varepsilon_1^2-\varepsilon_2^2+2\varepsilon_1\varepsilon_3\right) \quad \text{(A2)}$$

$$\frac{k_I^2}{k_0^2} = \frac{\begin{array}{c}\left(\varepsilon_1^2-\varepsilon_2^2\right)\sin^2(\theta)+\varepsilon_1\varepsilon_3\left(1+\cos^2(\theta)\right) \\ +\left[\left(\varepsilon_1^2-\varepsilon_2^2-\varepsilon_1\varepsilon_3\right)^2\sin^4(\theta)+4\varepsilon_2^2\varepsilon_3^2\cos^2(\theta)\right]^{1/2}\end{array}}{2\left[\varepsilon_1\sin^2(\theta)+\varepsilon_3\cos^2(\theta)\right]} \quad \text{(A3)}$$

$$\frac{k_{II}^2}{k_0^2}=\frac{\begin{array}{c}\left(\varepsilon_1^2-\varepsilon_2^2\right)\sin^2(\theta)+\varepsilon_1\varepsilon_3\left(1+\cos^2(\theta)\right)\\ -\left[\left(\varepsilon_1^2-\varepsilon_2^2-\varepsilon_1\varepsilon_3\right)^2\sin^4(\theta)+4\varepsilon_2^2\varepsilon_3^2\cos^2(\theta)\right]^{1/2}\end{array}}{2\left[\varepsilon_1\sin^2(\theta)+\varepsilon_3\cos^2(\theta)\right]} \tag{A4}$$

$$\frac{k_{zI}^2}{k_0^2}=\frac{\left[2\varepsilon_1\varepsilon_3-\frac{k_\rho^2}{k_0^2}(\varepsilon_1+\varepsilon_3)\right]+\left[\frac{k_\rho^4}{k_0^4}(\varepsilon_1-\varepsilon_3)^2+4\varepsilon_2^2\varepsilon_3\left(\varepsilon_3-\frac{k_\rho^2}{k_0^2}\right)\right]^{1/2}}{2\varepsilon_3} \tag{A5}$$

$$\frac{k_{zII}^2}{k_0^2}=\frac{\left[2\varepsilon_1\varepsilon_3-\frac{k_\rho^2}{k_0^2}(\varepsilon_1+\varepsilon_3)\right]-\left[\frac{k_\rho^4}{k_0^4}(\varepsilon_1-\varepsilon_3)^2+4\varepsilon_2^2\varepsilon_3\left(\varepsilon_3-\frac{k_\rho^2}{k_0^2}\right)\right]^{1/2}}{2\varepsilon_3} \tag{A6}$$

$$\hat{e}_{nI}(\pm k_{zI})=\frac{\bar{e}_I(\pm k_{zI})}{norm\left(\bar{e}_I(\pm k_{zI})\right)} \tag{A7}$$

$$\hat{e}_{nII}(\pm k_{zII})=\frac{\bar{e}_{II}(\pm k_{zII})}{norm\left(\bar{e}_{II}(\pm k_{zII})\right)} \tag{A8}$$

where

$$\bar{e}_I(\pm k_{zI})=\begin{bmatrix}1\\ \dfrac{A_{13}A_{21}+A_{23}\alpha_I-A_{23}A_{11}}{\alpha_I A_{13}-A_{22}A_{13}+A_{23}A_{12}}\\ \dfrac{-A_{12}}{A_{13}}\left[\dfrac{A_{13}A_{21}+A_{23}\alpha_I-A_{23}A_{11}}{\alpha_I A_{13}-A_{22}A_{13}+A_{13}A_{12}}\right]+\dfrac{\alpha_I-A_{11}}{A_{13}}\end{bmatrix} \tag{A9}$$

$$\bar{e}_{II}(\pm k_{zII})=\begin{bmatrix}1\\ \dfrac{A_{13}A_{21}+A_{23}\alpha_{II}-A_{23}A_{11}}{\alpha_{II}A_{13}-A_{22}A_{13}+A_{23}A_{12}}\\ \dfrac{-A_{12}}{A_{13}}\left[\dfrac{A_{13}A_{21}+A_{23}\alpha_{II}-A_{23}A_{11}}{\alpha_{II}A_{13}-A_{22}A_{13}+A_{13}A_{12}}\right]+\dfrac{\alpha_{II}-A_{11}}{A_{13}}\end{bmatrix} \tag{A10}$$

The coefficients in (A9)–(A10) are

$$A_{11}=\left(k_\rho^2+k_z^2\right)k_x^2-k_0^2\left[\varepsilon_1k_\rho^2+\varepsilon_3\left(k_x^2+k_z^2\right)\right]+k_0^4\varepsilon_1\varepsilon_3 \tag{A11}$$

$$A_{12}=\left(k_\rho^2+k_z^2\right)k_xk_y-k_0^2\left[i\varepsilon_2k_\rho^2+\varepsilon_3k_xk_y\right]+ik_0^4\varepsilon_2\varepsilon_3 \tag{A12}$$

$$A_{13}=\left(k_\rho^2+k_z^2\right)k_xk_z-k_0^2\left[\varepsilon_1k_xk_z+i\varepsilon_2k_yk_z\right] \tag{A13}$$

$$A_{21}=\left(k_\rho^2+k_z^2\right)k_xk_y-k_0^2\left[-i\varepsilon_2k_\rho^2+\varepsilon_3k_xk_y\right]-ik_0^4\varepsilon_2\varepsilon_3 \tag{A14}$$

$$A_{22}=\left(k_\rho^2+k_z^2\right)k_y^2-k_0^2\left[\varepsilon_1k_\rho^2+\varepsilon_3\left(k_y^2+k_z^2\right)\right]+k_0^4\varepsilon_1\varepsilon_3 \tag{A15}$$

$$A_{23}=\left(k_\rho^2+k_z^2\right)k_yk_z-k_0^2\left[\varepsilon_1k_yk_z-i\varepsilon_2k_xk_z\right] \tag{A16}$$

$$A_{31}=\left(k_\rho^2+k_z^2\right)k_xk_z-k_0^2\left[\varepsilon_1k_xk_z-i\varepsilon_2k_yk_z\right] \tag{A17}$$

$$A_{32} = \left(k_\rho^2 + k_z^2\right) k_y k_z - k_0^2 \left[\varepsilon_1 k_y k_z + i\varepsilon_2 k_x k_z\right] \quad \text{(A18)}$$

$$A_{33} = \left(k_\rho^2 + k_z^2\right) k_z^2 - k_0^2 \left[\varepsilon_1 \left(k_\rho^2 + 2k_z^2\right)\right] + k_0^4 \left[\varepsilon_1^2 - \varepsilon_2^2\right] \quad \text{(A19)}$$

where

$$k_\rho^2 = k_x^2 + k_y^2 \quad \text{(A20)}$$

REFERENCES

1. Bunkin, F. V., "On radiation in anisotropic media," *Sov. Phys. JETP, Engl. Transl.*, Vol. 5, 277–295, September 1957.
2. Wu, C. P., "Radiation from dipoles in an magneto-ionic medium," *IEEE Tran. Antennas Propag.*, Vol. 11, 681–689, November 1963.
3. Felsen, L. B. and N. Marcuvitz, *Radiation and Scattering of Waves*, Prentice Hall, New Jersey, 1973.
4. Clemmow, P. C., *The Plane Wave Spectrum Representation of Electromagnetic Fields*, Reissued edition, Chapter VIII, IEEE Press, New Jersey, 1996.
5. Alpert, Y. A. and B. S. Moiseyev, "On the distribution of the field electromagnetic waves emitted by a dipole in a homogeneous magnetoactive plasma," *J. Atmos. Terr. Phys.*, Vol. 42, 521–528, 1980.
6. Tai, C. T., *Dyadic Green's Functions in Electromagnetic Theory*, IEEE Press, 1994.
7. Eroglu, A. and J. K. Lee, "Dyadic Green's functions for an electrically gyrotropic medium," *Progress In Electromagnetics Research*, PIER 58, 223–241, 2006.
8. Eroglu, A. and J. K. Lee, "Wave propagation and dispersion characteristics for a non-reciprocal electrically gyrotropic medium," *Progress In Electromagnetics Research*, PIER 62, 237–260, 2006.
9. Bender, C. M. and S. A. Orszag, *Advanced Mathematical Methods for Scientists and Engineers*, 280–302, McGraw-Hill, New York, 1978.
10. Kong, J. A., *Theory of Electromagnetic Waves*, 59–62, 205–212, Wiley, New York, 1975.
11. Chew, W. C., *Waves and Fields in Inhomogeneous Media*, IEEE Press, 1995.
12. Courant, R. and D. Hilbert, *Methods of Mathematical Physics*, Vol. 1, Second Printing, Chapter VII, Interscience Publishers, New York, 1955.
13. Abramowitz, M. and I. Stegun, *Handbook of Mathematical Functions*, Chapter 9, 361, Dover Publications, New York, 1965.